Influence of Measurement Location on Transient Laser-Induced Incandescence Measurements of Particulate Matter in Raw Diesel Exhaust

Peter O. Witze
Sandia National Laboratories
Livermore, CA, USA 94551-0969

Gregory Payne and William D. Bachalo
Artium Technologies, Inc.
Sunnyvale, CA, USA 94086

Gregory J. Smallwood
National Research Council Canada
Ottawa, ON, CANADA K1A 0R6

Sub-Task 3.4S, *Year 2003 Annual Report of the International Energy Agency Program of Research in Energy Conservation and Emissions Reduction in Combustion*

ABSTRACT

Laser-induced incandescence can be applied to raw exhaust at the open tailpipe, or along the exhaust train using either an *in situ* optical cell or by extractive sampling to an external cell. While *in situ* measurements are preferable to avoid artifacts caused by extractive sampling, the experimental setup may be complex and thus more expensive to implement. In this paper we make a direct comparison of time-resolved *in situ* versus extracted-sample measurements for rapid engine transients of load and speed. In addition, we compare measurements for exhaust extracted from three different locations: 1) at the turbocharger output; 2) at the muffler entrance; 3) at the muffler exit. The results show that extractive sampling sufficiently replicates *in situ* measurements obtained at the muffler entrance, and that rapid transients in soot concentration vary to a small but detectable degree with the measurement location.

INTRODUCTION

Laser-induced incandescence (LII) has been shown over the past few years to be a valuable measurement technique for diesel particulate matter (PM) emissions. A high-energy, pulsed laser is used to heat the PM to very high temperatures, resulting in blackbody radiation that is proportional to the volume concentration of elemental carbon (EC). The EC component of PM is also referred to as soot. Key advantages of LII over more established, conventional techniques, are the ability to make real-time measurement in raw exhaust (i.e., without dilution) with high sensitivity (detection to better than one part-per-trillion [1]). In addition, because an LII system is virtually maintenance free, it is possible to run continuously, producing an analog-out signal suitable for a conventional, emissions data-acquisition system.

Since LII can be applied to raw exhaust, *in situ* measurements are possible. Application to an open, tailpipe exhaust is relatively easy to implement, but inline measurements such as the entrance to a particulate filter require optical access that can be both expensive and cumbersome. A much easier approach is to extract exhaust through a sampling line to an external optical cell. In this paper we present a direct comparison of LII measurements obtained *in situ* and by extraction. We also compare measurements for three different extraction locations, and in the appendix report some preliminary efforts for obtaining crank-angle-resolved LII measurements.

EVOLUTION OF LII

The early research using LII focused on planar (PLII) imaging of soot distributions in stationary flames [2-4]. PLII was also applied to in-cylinder studies of diesel combustion [5-7], and played an instrumental role in our current understanding of the structure and chemistry of burning diesel jets [8]. More recently, LII has seen extensive development as a highly-sensitive, real-time diagnostic for reciprocating engine PM emissions. Because, in general, the PM in engine exhaust is spatially homogeneous, planar imaging is unnecessary, and is supplanted by single-point detection techniques using fast photodiodes or photomultiplier tubes. Typically, a probe volume defined by the collimated laser beam and the collection optics is imaged onto the detector. A large probe volume is preferred, so that the measurement from a single laser pulse is essentially global and statistically representative of the exhaust soot concentration even at very low concentrations. A large probe volume also enhances the lower detectability limit and improves the signal-to-noise ratio with regard to unwanted elastic scattering from the walls of the optical cell.

Three research groups have been particularly active in the development of LII for reciprocating engine exhaust measurements, located at the Friedrich-Alexander-Universität, Erlangen-Nürnberg [9-11], the National

Research Council (NRC) Canada [12-14], and the Sandia National Laboratories [15,16]. The group in Germany is affiliated with a private company, Esytec Gmbh, which has offered a commercial LII instrument for several years [17]. The groups at NRC and Sandia also have commercialization as a goal, and are partnering with a private company, Artium Technologies, Inc., to produce a commercial instrument [18]. Finally, a group at Argonne National Laboratory is also working toward commercialization of an LII instrument for exhaust measurements [19].

EXPERIMENTAL

The LII instrument, the optical cells, sampling lines, and associated computer and electronics were configured for portability and ease of implementation, allowing rapid set-up in an engine or vehicle laboratory and only requiring access to a single electrical circuit. Details of the components are discussed below.

LASER-INDUCED INCANDESCENCE

The measurements to be reported in this paper were obtained during evaluation of a prototype Artium Technologies LII instrument, *LII 200*. The work was performed at Sandia using existing diesel laboratory facilities that include both *in situ* and external optical cells. The Artium instrument tested is unique in comparison to the other instruments mentioned in that it utilizes a technique patented by NRC [20] that permits quantitative measurements of soot concentration by a simple, *in situ* calibration with a tungsten lamp. Furthermore, the technique utilizes two-color pyrometry to measure the absolute soot temperature for each laser pulse. This has the added advantage of permitting the laser heating of the soot to be kept below the sublimation temperature. Conventional LII techniques require the measurements to be performed at or above the sublimation temperature to eliminate the dependence of the LII signal intensity on the laser fluence (energy per unit area of the laser beam). Unfortunately, sublimation causes an unknown amount of material loss during the measurement interval that can compromise the accuracy of the results.

The Artium *LII 200* instrument used in these investigations consists of a self-contained rugged optics enclosure which includes the laser and all components needed for operation of the instrument. The optical system consists of a computer-controlled automated laser beam energy detection and adjustment system that maintains the laser light fluence at the sampling volume at optimum conditions. Optics are provided to transform the laser beam intensity into a near top-hat profile which facilitates uniform heating of the soot in the sample volume. Incandescence signal detection is made at 90 degrees to the transmitted beam which helps form a well-defined measurement volume. The incandescence signal is detected by a pair of detectors that use light filters centered at wavelengths of approximately 400 and 800 nanometers. Among other advantages, this allows the use of the two-color pyrometry technique to measure soot particle temperature after laser light heating and during the measurement interval. This information is also used internally to automatically adjust the laser fluence to the appropriate value to achieve a maximum soot temperature at just below temperatures at which sublimation becomes significant. Computer-controlled photomultiplier gain and signal attenuation allow consistent operation over a very wide range of soot concentration without any user intervention.

A custom 2-channel 12 bit, 100 MHz PCI A/D digital signal acquisition card is used for optimized high-speed data acquisition and transfer to the computer. A USB interface between the *LII 200* optics package and the system computer is used for the control functions. The system software, which controls all aspects of the instrument setup and operation, runs on either Windows (2000/XP) or Linux (2.4 kernel) and is designed around a client/server architecture allowing remote operation via intranet or Internet and secure multi-user access. Algorithms are included for automated setup of the instrument functions and online adjustment to the prevailing measurement conditions. An external input feature allows tagging of the LII signals with the engine operating parameters (i.e. speed, load, etc.). The instrument has the capability of accepting, processing, displaying, and storing data for extended periods of time without interruption. During long acquisition periods, the data can be broken into multiple files (e.g., one file per hour) for greater manageability. The data analysis and display are easily extensible and may be modified as needed. The data can be easily exported to Microsoft Excel for further analysis and custom display.

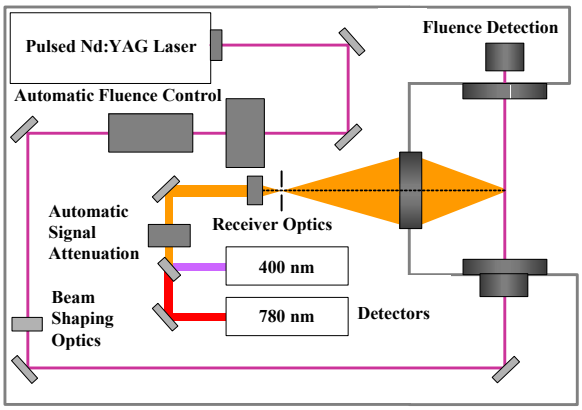

Figure 1: Schematic of the optical arrangement of the LII instrument.

OPTICAL CELLS

The optical cell we use for the extracted-sample measurements is shown in Fig. 2. It was designed with general-purpose use in mind, to permit both the development of new diagnostic techniques and the application of commercial instrumentation such as the LII instrument shown in Fig. 1.

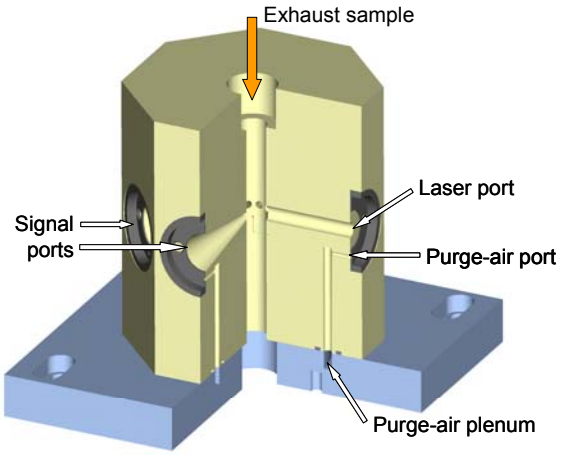

Figure 2: Schematic of the external optical cell for extracted exhaust measurements.

The octagonal flow chamber contains six conic viewing ports (21° solid angle) and two opposing cylindrical ports (5.7 mm diameter) for transmission of the laser beam. The flow passage is 10.2 mm in diameter. Imbedded electrical heaters maintain the cell temperature at 90 °C. The windows are mounted in commercial lens tubes that attach directly to the optical cell. The windows are kept clean by an air-purge system consisting of a common annular plenum in the base plate, connected by individual passages to the laser and signal ports. An aquarium aerator pump is used to provide a purge air flow rate of 20 ml/m, 0.1% of the exhaust-sample flow rate. As such, the window air purge has an insignificant effect on the measured soot concentration.

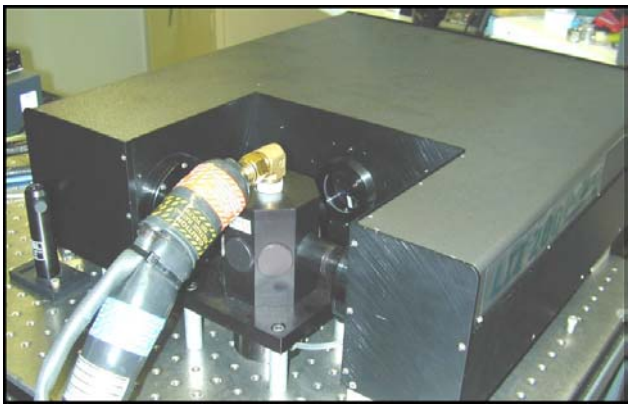

Figure 3: LII instrument with the external optical cell for extracted exhaust measurements.

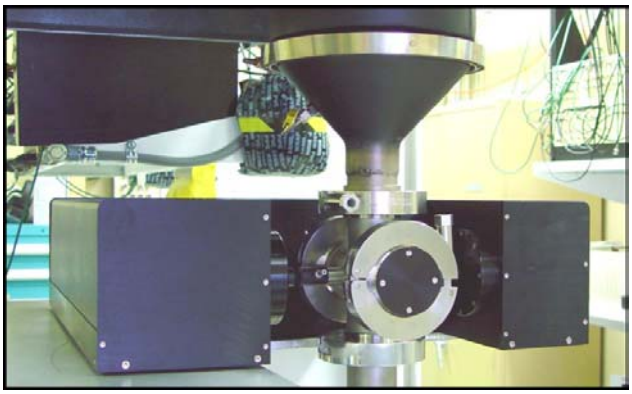

Figure 4: LII instrument with the *in situ* optical cell.

The optical cell is mounted to a 2'x3' breadboard attached to the top shelf of a 2'x4' mobile cart. The LII instrument sits on the breadboard, as shown in Fig. 3. Adjustable lens tubes are used to enclose the laser beam path between the optical cell and the LII instrument, preventing the escape of stray laser light. The pump to draw the exhaust sample sits on a lower shelf of the cart, together with the laser power supply and PC. Also shown in the figure is the end of the 4' heated line that connects to the extraction point at the engine. All ancillary equipment is also mounted on the cart, creating a single-piece, self-contained, portable system. Implementation simply requires connecting the extraction and vent lines, and plugging into a 120V receptacle.

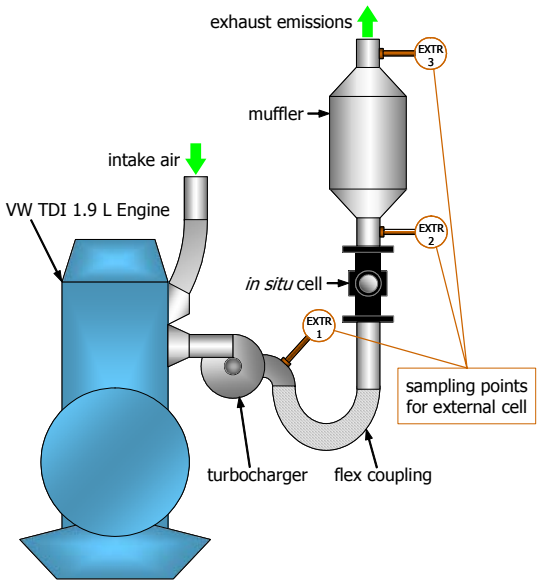

Figure 5: Measurement locations for LII instrument.

The *in situ* optical cell is designed with similar concepts as the external cell, except that machining costs were minimized by using a vacuum-flange 4-way cross with 2" ID for the main body of the cell. One branch of the cross was used for the exhaust stream, and the other to collect the signal, as shown in Fig. 4. (For the present application we closed off the second available signal

port.) An insert in the signal port converted the cylindrical passage into a cone of 21° solid angle, to minimize the size of the viewing aperture in the wall of the exhaust passage. To accommodate the laser beam, two tubes were brazed to the sides of the cross. An air purge was again used to keep the windows clean, but no preheating of the cell was used. The *in situ* cell was located in-line between the turbocharger exit and the muffler entrance, as indicated in Fig. 5. An adjustable shelf permitted positioning the LII instrument at the window level.

ENGINE FACILITY AND OPERATING PROCEDURE

The measurements to be reported were made on a 1996 Volkswagen 1.9-L TDI diesel engine. The stock engine control module (ECM) was used for primary engine-control management. However, we established auxiliary control capabilities with a laboratory PC for the accelerator pedal position, EGR control valve position, and water-brake load. For the first set of experiments, where we investigate the effect of measurement location for transient engine operation, we ran three transient sequences as summarized in Table 1. The EGR level was under ECM control for all experiments. For the free-acceleration sequence the water brake was disabled. The sequences were controlled by the PC and repeated continuously. The number of engine cycles for each state of a sequence was selected to reach approximately-steady performance. However, because the focus of our interest was transients, we did not desire lengthy periods of near-steady performance.

Table 1 Transient Engine-Operation Sequences

Sequence	State	#Cycles	Accel. Pos. (%)	RPM
Free Accel.	Off	150	0	830
	On	75	28	NA
Loaded Accel.	Off	150	0	830
	On	75	28	1500
Load Change	Low	175	23	1500
	High	125	35	1500

Included with the manufacturer's stock, on-board instrumentation on this engine is a needle-lift sensor located on the #3 cylinder. The sensor is normally used by the ECM to monitor injection timing, but we were also able to monitor the signal to determine the injection scheme used during decelerations. We found that for the deceleration at the end of the free acceleration, the injector was turned off for an average of 13 cycles, whereas for the deceleration at the end of the loaded acceleration it was turned off for only one or two cycles, and it remained on throughout the load change sequence.

During warm-up and between transient experiments, the engine was operated steady-state at a moderate load condition. When a transient sequence was initiated, we would repeat the sequence for several minutes to reach quasi-steady thermal conditions before enabling data acquisition. We then recorded the LII and PC command signals, as well as the engine speed for a 3 minute period at a 20 Hz data rate.

RESULTS

Measurements for the complete 3 minute experimental sequence for the free acceleration are presented in Fig. 6. The LII measurements shown were made *in situ*. Presenting the engine speed data in this fashion gives some insight into the repeatability of the engine performance. The LII measurements have the appearance of being "noisy", when in fact they reflect the rapid fluctuations in soot concentration in the LII probe volume.

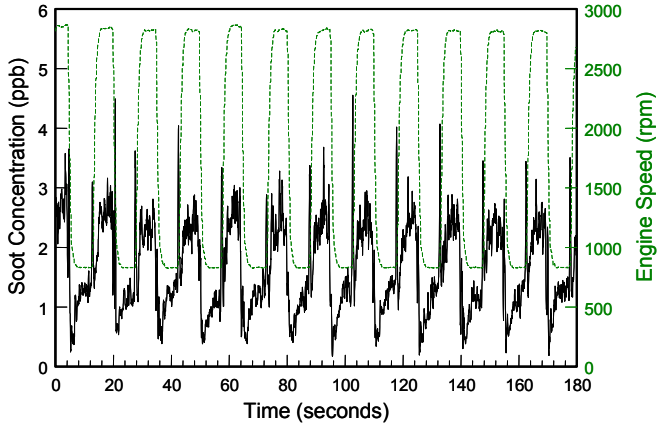

Figure 6: Free-acceleration experimental sequence showing engine speed and soot concentration by LII.

To better visualize the transient behavior of the exhaust PM, we show in Fig. 7 the LII measurements ensemble-averaged for the 10 cycles captured in the sequence. No attempt was made to correct the phasing of the time base to account for the lag between the engine speed measurement and the time required for the exhaust flow to reach the cell. We use the PC square-wave command that toggles the events in the sequence to establish the phasing, and do this for both the "on" and "off" commands to optimize the phase locking. In addition, because these raw ensemble measurements still exhibit significant fluctuations, we apply a smoothing procedure where we plot the average of every 5-adjacent points. As seen in Fig. 7, this has only a moderate effect on the amplitude of the largest excursions in the transient measurements.

The LII measurements presented in Fig. 7 reveal an abrupt burst of soot in response to the accelerate command, followed by a return to the initial level and then a more gradual rise to a plateau that appears to approach an asymptote toward the end of the high speed interval. A corresponding rapid reduction of soot

is seen to occur when fuel injection is interrupted at deceleration. As mentioned earlier, fuel injection is disabled by the ECM for an average of 13 engine cycles for this free-acceleration experiment. Assuming an average speed of 2000 rpm, this corresponds to slightly less than one second, which is of the order of the corresponding observed soot decay period. This is followed by another rapid burst of soot that we suspect is due to the resumption of fuel injection. From this point there is a more gradual decline to a minimum before an increase at a slower rate, approaching an asymptote near the initial soot concentration.

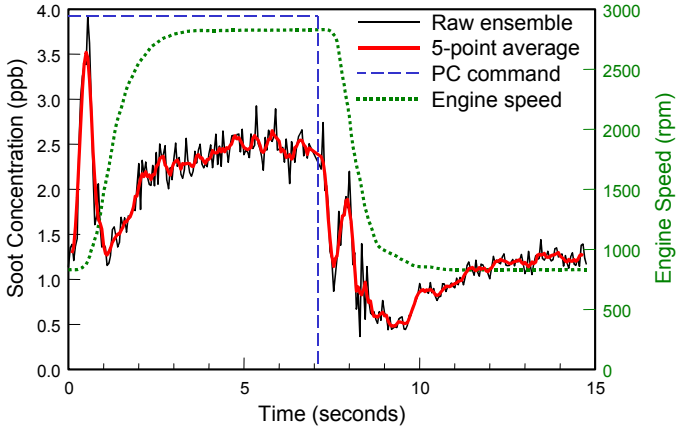

Figure 7: Ensemble average of free-acceleration results comparing the raw ensemble with a 5-point smoothing procedure.

IN SITU VERSUS EXTRACTION

The optical cells used for this study were not specifically designed for compatibility with the Artium LII instrument. As a consequence, the signal-collection ports of the external cell have a smaller geometric solid angle than the collection optics of the LII instrument, resulting in a loss of measured LII signal that necessitated the application of a correction factor to the magnitude of the LII measurements of extracted soot. Due to this clipping of the collected light, the external cell was also much more sensitive to misalignment than the *in situ* cell.

The *in situ* LII measurements for the free-acceleration experiment are shown in Fig. 8 compared with extracted sample results taken from just before the muffler, immediately downstream of the *in situ* cell (see Fig. 5). These and subsequent measurements report the 5-point average of ensemble averaged results for a sequence of 10 transient operations. The engine speed measurements for both experiments are shown, to illustrate engine performance repeatability. The extracted LII results are delayed in time relative to the *in situ* measurements because of the additional transit time of the exhaust gases from the extraction point to the external optical cell. Neither is compensated to align with the engine speed data.

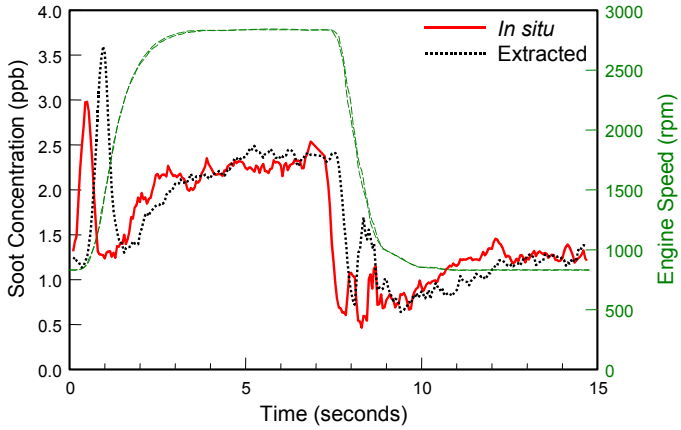

Figure 8: Comparison of *in situ* and extracted LII measurements for the free-acceleration experiment.

In Fig. 9 we show the extracted measurements empirically phase-shifted to align with the *in situ* results, and amplitude corrected as discussed earlier. The similarity of the measurements is excellent, particularly considering the difficulty of achieving identical engine performance for measurements taken many hours apart.

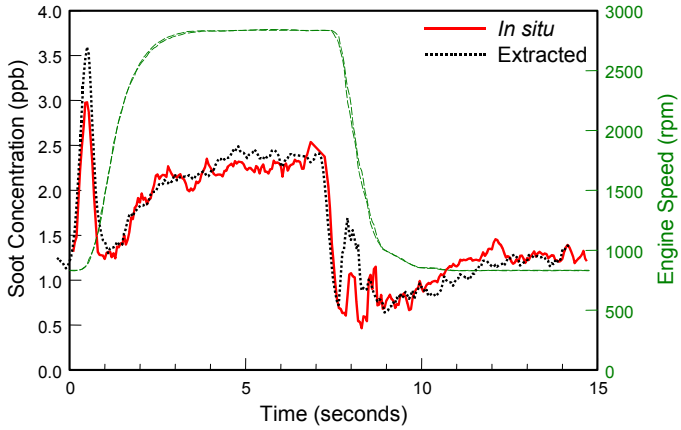

Figure 9: Comparison of phase-shifted *in situ* and extracted LII measurements for the free-acceleration experiment.

In Fig. 10 we show the comparison for the loaded-acceleration experiment described in Table I, where again we have phase-shifted the extracted measurements. We don't have an explanation for the differences in amplitude in the quasi-steady regions following the acceleration and deceleration transients. However, the general features of the transient soot concentration follow the same temporal behavior in both cases.

Because Figs. 9 and 10 reveal that there are significant differences in soot concentration between the free and loaded acceleration experiments, we compare them directly in Fig. 11. The behavior of the two results is seen to be quite similar immediately following the acceleration and deceleration commands. The higher

soot level for the free acceleration experiment after the acceleration is due to the higher engine speed. After the deceleration, the soot level for the loaded acceleration is higher because of the presence of a load. This is expected behavior.

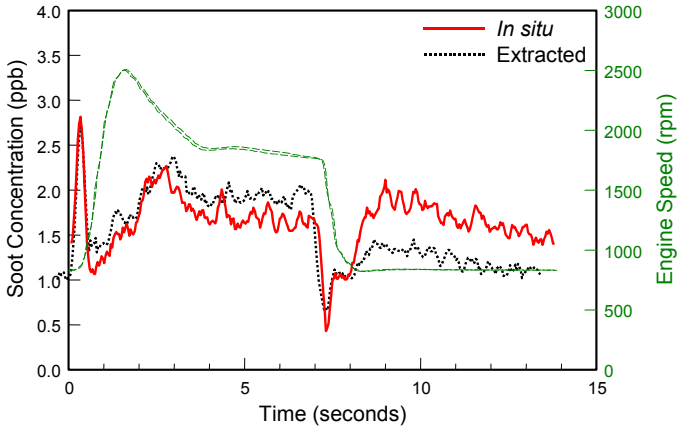

Figure 10: Comparison of phase-shifted *in situ* and extracted LII measurements for the loaded-acceleration experiment.

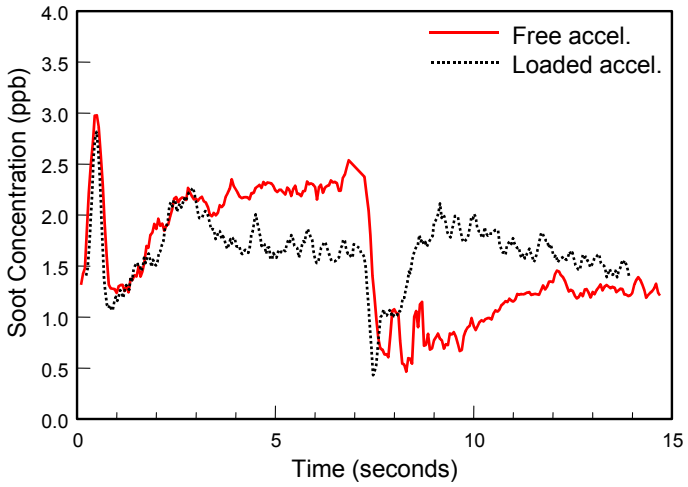

Figure 11: Comparison of the *in situ* free- and loaded-acceleration measurements.

Finally, in Fig. 12 we compare the in situ and extracted LII measurements for the load-change experiment. The agreement between the data using two methods of sampling the temporal behavior is very good, but the differences in level are troublesome. Coagulation would increase size with a reduction in number, but the volume fraction should stay constant. Adsorption of volatiles should not be an issue, because the intense laser light pulse used in the LII method will evaporate these components without detecting them. The three experiments at each location were run in succession, so there was no change in optical alignment.

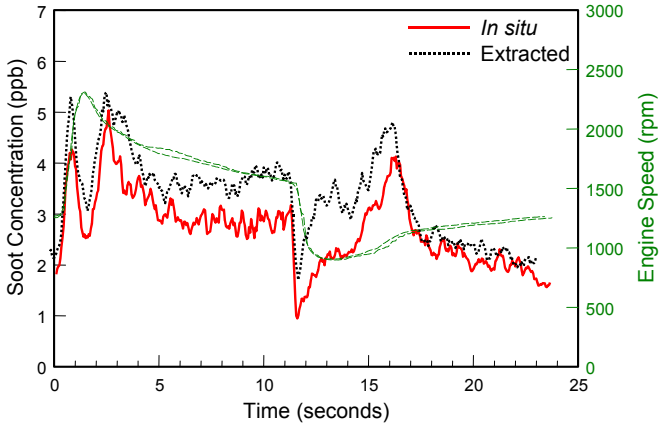

Figure 12: Comparison of phase-shifted *in situ* and extracted LII measurements for the load-change experiment.

EFFECT OF EXTRACTION LOCATION

Fig. 13 summarizes the extracted-sample measurements for the three extraction locations shown in Fig. 5 and the three transient experiments. (There are no measurements at the turbo exit for the loaded-acceleration experiment because a major mechanical failure on the engine terminated the study at this point.) A common observation for all three experimental conditions is that the time delay for soot-concentration transients to reach the extraction locations is apparent, but not always consistent (the muffler entrance is 147 cm from the turbo exit, and the muffler exit is 51 cm further). This variability is a direct result of the imprecise repeatability of the engine response to the transient sequences. Of course, the muffler acts as a damping chamber with a relatively large volume, so that the phasing of the transients may not reflect the linear path difference between the sampling locations. The muffler will damp the magnitude of the excursions of the transients. Furthermore, the higher surface-to-volume ratio, lower velocities, and increased thermophoresis will all lead to increased deposition in the muffler, lowering the anticipated soot concentration at the muffler exit location.

For both the free and loaded acceleration, the burst of soot at the start of the transients is measurably lower at the muffler exit compared to the other locations, whereas this is not the case for the load change. For the remainder of the experimental periods the soot levels are quite similar at all locations with two exceptions. First, for the high speed portion of the free acceleration (Fig. 13a) the soot concentration at the muffler exit is considerably lower than at the other two locations, whereas for the low speed portion the muffler entrance and exit concentrations are similar but lower than at the turbo exit. Second, following the load change in Fig. 13c there are significant differences in soot concentration for all three locations, with a consistent trend of lower soot with distance from the engine. This is consistent with deposition of the soot particles along the pathway from

the engine, with the greatest deposition occurring in the muffler.

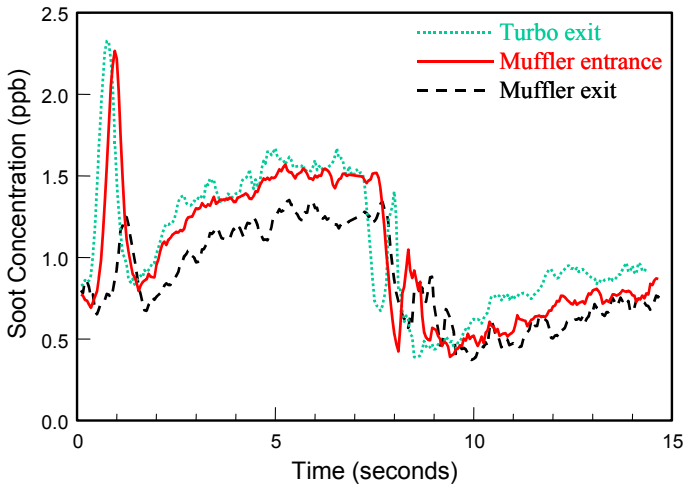

a.) Free acceleration

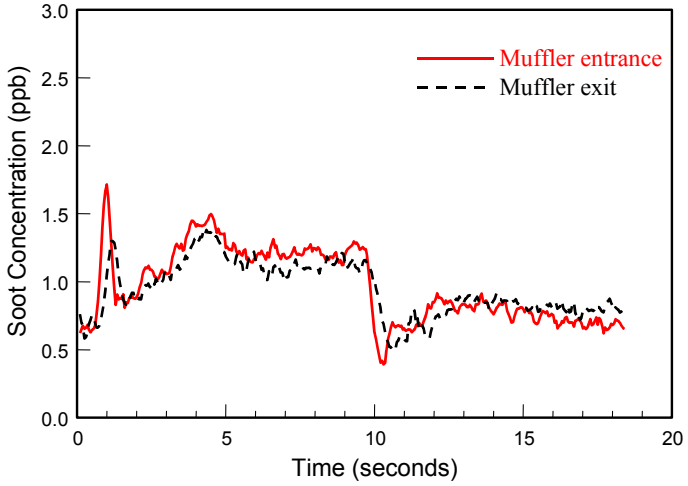

b.) Loaded acceleration

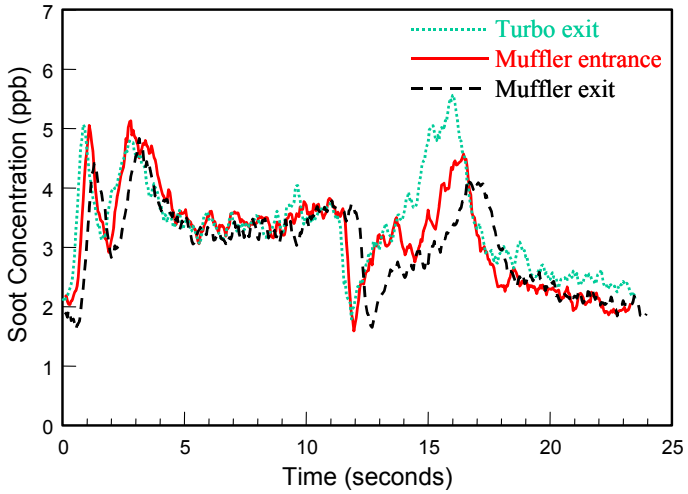

c.) Load change

Figure 13: Effect of extraction location on LII measurements of soot concentration.

CONCLUSIONS

Considering the difficulty in achieving closely repeated conditions, it would appear that soot concentration does not change significantly during passage through the exhaust system. As LII is insensitive to coagulation and desorption, it is likely that any changes observed are due to deposition on the walls. There also is negligible loss in temporal behavior between *in situ* and extracted measurements. Some differences in concentration were observed, which are likely due to diffusion, damping of transients, and mixing in the streamwise direction.

Given the number of possibilities for variance in the soot emissions, the results were in good agreement and the trends were clearly identifiable. We have evaluated the LII method under steady state conditions and have found excellent precision in the measurements. Variations over extended periods of time were much smaller than the variance seen in the present results. Thus, it may be concluded that the variations in the data were due to the source (changes in the engine conditions, exhaust system, and sampling devices). Nonetheless, the results provide useful information of the transient emissions characteristic of diesel engines, whether *in situ* sampling or extractive sampling is used.

ACKNOWLEDGMENTS

This work was performed at the Combustion Research Facility, Sandia National Laboratories, Livermore, CA. The Sandia contribution was funded by the U.S. Department of Energy, Office of FreedomCAR and Vehicle Technologies under the direction of Gurpreet Singh. The Artium contribution was funded by NASA Glenn Research Center under SBIR Phase I-III contracts, and by the U. S. EPA under SBIR Phase I and Phase II contracts. The NRC contribution was funded by the Particulates POL of the Canadian Government's PERD Program.

REFERENCES

1. Wainner, R. T., Seitzman, J. M. and Martin. S. R., "Soot Measurements in a Simulated Engine Exhaust using Laser-Induced Incandescence," *AIAA J.* **37**, No. 6, pp. 738-743, 1999.
2. Vander Wal, R. L. and Weiland, K. J., "Laser-Induced Incandescence: Development and Characterization Towards a Measurement of Soot Volume Fraction," *Appl. Phys. B* 59:445-452, 1994.
3. Shaddix, C. R and Smyth, K. C., "Quantitative Measurements of Enhanced Soot Production in Steady and Flickering Methane/Air Diffusion Flame," *Comb. and Flame* 99:723-732, 1994.
4. Ni, T., Pinson, J. A., Gupta, S. and Santoro, R. J., "Two-Dimensional Imaging of Soot Volume Fraction by the Use of Laser-Induced Incandescence," *Appl. Opt.* 34:7083-7091, 1995.

5. Dec., J. E., zur Loye, A. O. and Siebers, D. L., "Soot Distribution in a D. I. Diesel Engine Using 2-D Laser-Induced Incandescence Imaging," SAE Paper No. 910224, 1991.
6. Won, Y-H., Kamimoto, T., Kobayashi, H. and Kosaka, H., "2-D Soot Visualization in Unsteady Spray Flame by means of Laser Sheet Scattering Technique," SAE Paper No. 910223, 1991.
7. Pinson, J. A., Mitchell, D. L., Santoro, R. J. and Litzinger, T. A., "Quantitative, Planar Soot Measurements in a D.I. Diesel Engine Using Laser-Induced Incandescence and Light Scattering," SAE Paper No. 932650, 1993.
8. Dec, J. E., "A Conceptual Model of DI Diesel Combustion Based on Laser-Sheet Imaging," SAE Paper No. 970873, 1997.
9. Schraml, S., Will, S., and Leipertz, A., "Simultaneous Measurement of Soot Mass Concentration and Primary Particle Size in the Exhaust of a DI Diesel Engine by Time-Resolved Laser-Induced Incandescence (TIRE-LII)," SAE Paper 1999-01-0146, 1999.
10. Schraml, S., Will, S., Leipertz, A., Zens, T., and D'Alfonso, N., "Performance Characteristics of TIRE-LII Soot Diagnostics in Exhaust Gases of Diesel Engines," SAE Paper No. 2000-01-2002, 2000.
11. Schraml, S., Heimgärtner, C., Will, S., Leipertz, A., and Hemm, A., "Application of a New Soot Sensor for Exhaust Emission Control Based on Time Resolved Laser Induced Incandescence (TIRE-LII)," SAE Paper No. 2000-01-2864, 2000.
12. Snelling, D. R., Smallwood, G. J., Sawchuk, R. A., Neill, W. S., Gareau, D., Clavel, D., Chippior, W. L., Liu, F., Gülder, Ö. L. and Bachalo, W. D., "Particulate Matter Measurements in a Diesel Engine Exhaust by Laser-Induced Incandescence and the Standard Gravimetric Procedure," SAE Paper No. 1999-01-3653, 1999.
13. Snelling, D. R., Smallwood, G. J. and Gülder, Ö. L., "Soot Volume Fraction Characterization Using the Laser-Induced Incandescence Detection Method," Proceedings of the 10th International Symposium on Applications of Laser Techniques to Fluid Mechanics, Lisbon, 2000.
14. Smallwood, G. J., Snelling, D. R., Neill, W. S., Liu, F., Bachalo, W. D., and Gülder, Ö. L., "Laser-Induced Incandescence Measurements of Particulate Matter Emissions in the Exhaust of a Diesel Engine," Proceedings of the Fifth International Symposium on Diagnostics and Modeling of Combustion in Internal Combustion Engines (COMODIA), Nagoya, 2001.
15. Witze, P. O., "Qualitative Laser-Induced Incandescence Measurements of Soot Emissions During Transient Operation of a Port Fuel-Injected Engine," Proceedings of the Fifth International Symposium on Diagnostics and Modeling of Combustion in Internal Combustion Engines (COMODIA), Nagoya, 2001.
16. Axelsson, B., and Witze, P. O., "Qualitative Laser-Induced Incandescence Measurements of Particulate Emissions During Transient Operation of a TDI Diesel Engine," SAE Paper No. 2001-01-3574.
17. http://www.esytec.de/englisch/index_engl.htm.
18. http://www.ca.sandia.gov/pmc.
19. http://transtech.anl.gov/v1n4/tgi-instrument.html.
20. Snelling, D. R., Smallwood, G. J. and Gülder, Ö. L., "Absolute Light Intensity Measurements in Laser Induced Incandescence," US Patent No. 6,154,277, 2000.
21. Dec, J. E. and Kelly-Zion, P. L., "The Effects of Injection Timing and Diluent Addition on Late-Combustion Soot Burnout in a DI Diesel Engine Based on Simultaneous 2-D Imaging of OH and Soot," SAE Paper No. 2000-02-0238, 2000.
22. Reitz, R. D., U. of Wisconsin, private communication.
23. Green, R. M., "Measuring the Cylinder-to-Cylinder EGR Distribution in the Intake of a Diesel Engine During Transient Operation," SAE Paper No. 2000-01-2866, 2000.
24. http://www.cambustion.co.uk.
25. Henein, N. A., Tagomori, M. K., Yassine, M. K., Henien, H. A., Hartman, P. and Asmus, T., "In-Situ Phase-Shift Measurement of the Time-Resolved UBHC Emissions, SAE Paper No. 950161, 1995.

APPENDIX – CRANK-ANGLE RESOLVED LII

There is reason to expect that crank-angle-resolved, cylinder-out PM measurements may be important to the understanding of in-cylinder soot formation mechanisms. For example, Dec and Kelly-Zion [21] used planar imaging by LII to investigate incomplete burnout in the bulk gases of a heavy-duty diesel engine. They observed inhomogeneous soot pockets that tend to follow the piston down during the first part of the expansion, rather than expanding uniformly. Crank-angle-resolved LII measurements in the exhaust port could resolve this phenomena, avoiding the need for optical access to the cylinder.

As another example, the high swirl and reentrant piston bowl characteristic of small-bore, high speed diesel engines creates an environment for inhomogeneous in-cylinder soot distributions. Computational fluid mechanics investigations predict unoxidixed soot pockets trapped in the piston bowl [22], such that crank-angle resolved measurements of PM flux in the exhaust port could be valuable for model validation.

Although obtaining optical access to the exhaust port is far easier than in-cylinder access, it is not a trivial task. In addition, for two-valve-per-cylinder engines such as the one used here, it is not uncommon to have adjacent intake and exhaust manifolds (on the same side of the block) that make optical access even more difficult. Green [23] modified both manifolds on the engine used in the present study to obtain optical access to all four intake runners to develop an absorption technique for the measurement of cylinder-to-cylinder EGR distribution. Because the cost and time required to modify the manifolds was substantial, future applications of the technique were performed with an optical probe that was inserted into the intake runner.

An alternative approach is to continuously extract a sample of the flow to an external measurement location, such as the

Cambustion fast-response flame ionization detector [24] for measuring unburned hydrocarbon (UHC). With this instrument, a gas sample is extracted from the exhaust port through a fine capillary tube (typically 0.5 mm ID) to the ionizing flame. Because very little mixing occurs in the streamwise direction, fast response times are observed (10-90% of full scale in typically 4 ms). The transit time for the sample to flow from the pickup point in the exhaust port to the flame can be measured directly using the procedure described by Henein, et al. [25], where a nitrogen jet was used to abruptly interrupt the UHC concentration of the extracted sample.

Unfortunately, capillary-sized sampling lines are not compatible with the larger measurement volumes required for optimal LII measurements. The use of larger diameter sample lines thus raises the question of whether mixing along the extraction path to the optical cell severely compromises the achievable temporal resolution. In the remainder of this Appendix we assess the possible of making crank-angle-resolved LII measurements using extractive sampling techniques.

TEMPORAL RESPONSE ESTIMATE

Fig. 14 illustrates the flow setup we used to emulate the previously mentioned procedure of Henein et al. [25]. A 15 cm length of ¼" stainless steal tubing was inserted through the exhaust manifold to within a centimeter of the exhaust valves. This piece of tubing was connected to a 100 cm length of similar tubing with a compression "tee" fitting. This longer line was heated to 90 °C and connected to the optical cell. Clean nitrogen at 400 kPa was intermittently delivered to the 90-degree branch of the "tee" through a fast-acting solenoid valve.

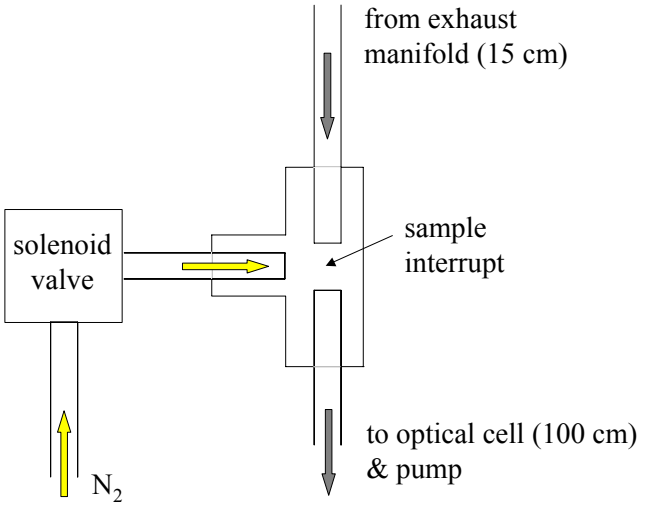

Figure 14: Flow setup for synchronous interruption of the exhaust flow by a nitrogen jet.

With the engine running at 1500 rpm (80 ms/cycle), our procedure was to open the solenoid valve every 20 engine cycles for a duration of 5 engine cycles. The sequencing of the solenoid valve was controlled by the same PC software that provided the engine transients reported earlier in this paper. Shown in Fig. 15 are synchronous LII measurements made at TDC of the compression stroke for an ensemble-average of 10 injection sequences. Unlike the calibrated LII measurements presented in the first section of this paper, the data shown here are simply the maximum of the LII signal in volts. It is seen that it takes two engine cycles for the effect of the nitrogen jet to achieve approximately 90% of the asymptotic values for both jet-on and jet-off.

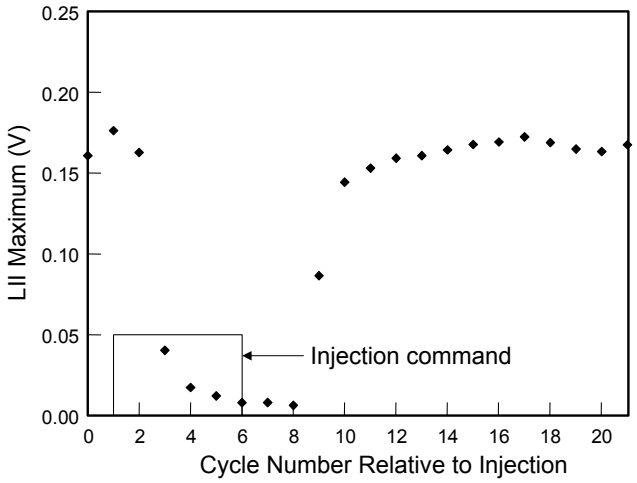

Figure 15: Synchronous LII measurements for the nitrogen-injection sequence.

Note, however, the unusually high value for the LII measurement for cycle #1. This is due to an increase in the exhaust gas density in the optical cell caused by the 400 kPa supply pressure for the nitrogen. (The nitrogen injection command occurred at TDC of valve overlap; the LII measurements were taken one-half cycle later at TDC of compression/expansion.) This explanation is confirmed by the crank-angle resolved LII measurements for the second injection cycle shown in Fig. 16, which reveal a distinct oscillation in the PM concentration caused by pressure waves.

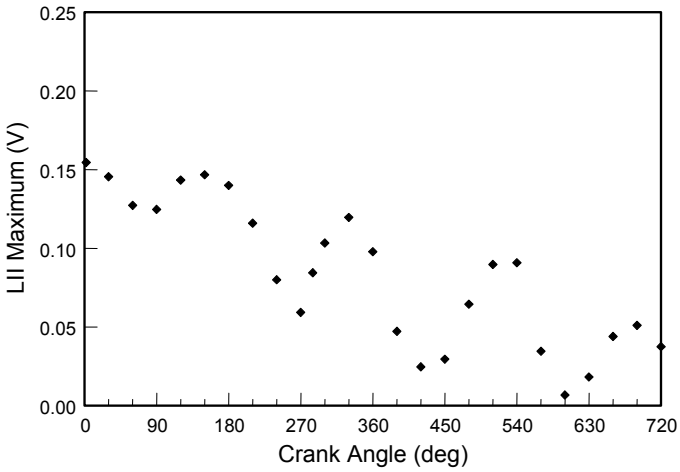

Figure 16: Crank-angle resolved LII measurements for the second nitrogen-injection event.

The flow rate for the extracted sample in Figs. 15 and 16 was 5 lpm. By increasing it to 10 lpm we significantly dampened the pressure oscillations, as shown by the crank-angle resolved LII measurements in Fig. 17 for the initial part of the injection sequence.

Based on a simple bench top deflection experiment, we estimated that the nitrogen jet arrives at the gap in the sampling line 16 ms after the command to open the solenoid valve. From this point, the data in Fig. 17 show a transit time through the 100 cm line to the optical cell of 335 crank-angle degrees (37 ms). Assuming simple plug flow, this corresponds to an average flow rate of 2.7 lpm during this interval, as compared to the set, steady-state flow rate of 10 lpm. This confirms that the transit time to the optical cell is strongly

influenced by the high pressure of the nitrogen supply. However, we chose to use a high pressure to insure a rapid interruption of the PM concentration in the sample flow. The results shown in Fig. 17 imply a response time on the order of 60-90 crank-angle degrees. While this is marginal, at best, it would seem to be adequate to observe some transient behavior during blowdown and exhaust.

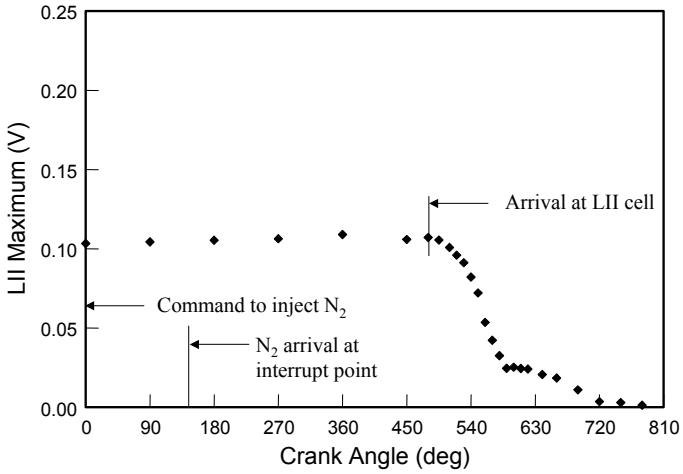

Figure 17: Crank-angle resolved LII measurements of the exhaust flow interrupted by a nitrogen jet.

TEMPORAL RESPONSE RESULTS

Presented in Fig. 18 are crank-angle resolved LII measurements for one complete engine cycle, recorded with 30 crank-angle-degree resolution. The sample flow rate was 20 lpm, and each data point represents an ensemble-average of 100 laser pulses. The straight line is the average of all the measurements, and reveals that there is no noticeable transient behavior in the results. We took some measurements at other sample flow rates with similar results.

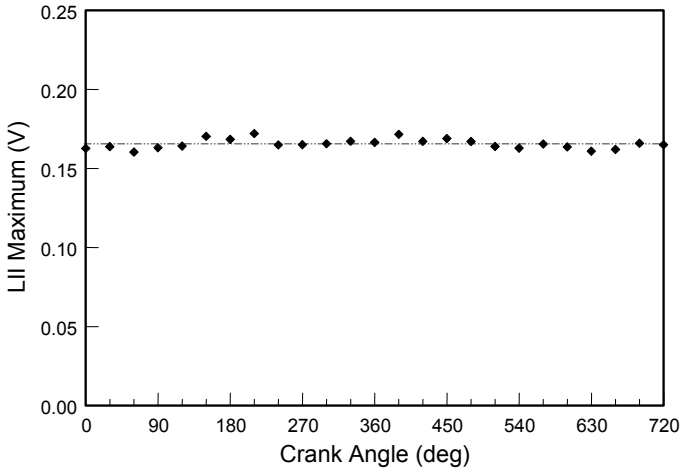

Figure 18: Crank-angle resolved LII measurements of the exhaust flow for the configuration described in Fig. 16 (115 cm line length).

In a last attempt to resolve transient behavior within an engine cycle, we moved the optical cell to as close to the engine as possible, as shown in Fig. 19. The total sample line length was 30 cm, and it was necessary to have a 90-degree elbow in the line. Because of vibration of the engine, it was not possible to use a PMT to detect the LII signal. In its place we used a small photodiode that could be mounted directly to the optical cell. This resulted in significantly lower LII signal levels.

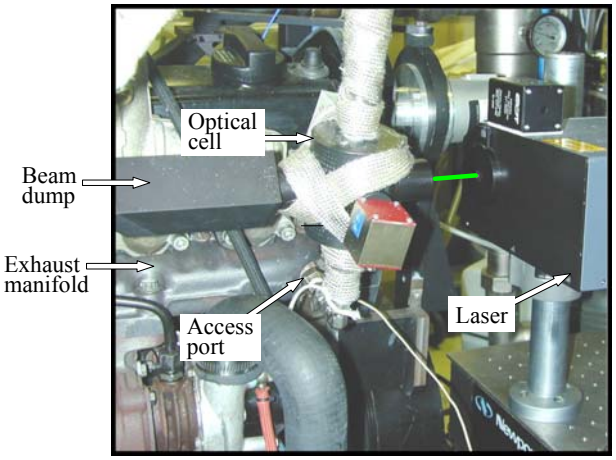

Figure 19: Position of the close-coupled optical cell.

LII measurements for the close-coupled optical cell are given in Fig. 20 for flow rates of 10 and 20 lpm. Because there was much less transient behavior for the former, results are shown for 90 crank-angle-degree resolution, whereas for the latter 10 degree resolution is used. For plug flow at 20 lpm, and nominal exhaust valve opening at –180 crank-angle degrees, the exhaust event is calculated to reach the sampling cell at –45 crank-angle degrees, which is in reasonable agreement with the beginning of the LII transient. This suggests that the increase in LII signal at this time is most likely due to an increase in PM concentration, and not an artifact of a density increase associated with a pressure increase at blowdown.

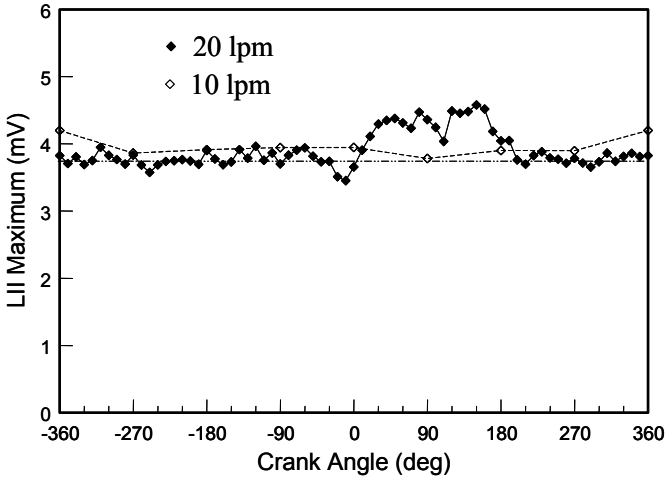

Figure 20: Crank-angle resolved LII measurements for the close-coupled optical cell.

Thus, in this preliminary effort, it appears that it is possible to measure transient crank-angle resolved soot concentrations with LII. However, further effort is required to optimize the conditions for close-coupled sampling.